文章编号：1001-9014(2021)02-0243-05

DOI: 10.11972/j.issn.1001-9014.2021.02.015

The method of dispersion cancellation based on the forward and reverse tuning of a laser frequency-modulated continuous wave system

XU Xin-Ke, LONG Kang, XU Jing-Xiang, ZHAO Jun, WANG Dao-Dang, LIU Lu, LIU Wei, GUO Tian-Tai, KONG Ming*

(College of Metrology and Measurement Engineering, China Jiliang University, Hangzhou 310018, China)

Abstract: To reduce the dispersion mismatch effect on FMCW measurements, a method of eliminating dispersion mismatch by the forward and reverse tuning of an external cavity tunable laser is proposed. When the external cavity tunable laser is combined with an optical fiber path, the system produces a dispersion mismatch effect, which is manifested as peak broadening and shifting of the target signal. The ranging value changes with the increase in the tuning bandwidth, resulting in measurement instability. To solve this problem, the paper studies the system dispersion mismatch characteristics of the external cavity tunable laser in forward and reverse tuning. The results show that the dispersion trend is a symmetrical distribution of the forward and reverse tuning. The paper establishes the dispersion mismatch model of the forward and reverse tuning system. On this basis, dispersion cancellation is realized by forward and reverse tuning of the external cavity laser. This method does not require calibration of the dispersion coefficient of the system in advance nor cyclic iterative compensation. A single measurement can complete the dispersion compensation for the system, which provides a way to improve the efficiency of dispersion compensation.

Key words: optics, laser frequency modulated continuous wave (FMCW), laser ranging, dispersion compensation, external cavity tunable laser

PACS: 42.25.Hz, 07.60.Vg, 42.79.Qx, 81.05.Ni

基于激光调频连续波正反向调谐色散对消方法

许新科，龙 康，徐靖翔，赵 军，王道档，刘 璐，刘 维，郭天太，孔 明*

（中国计量大学 计量测试工程学院，浙江 杭州 310018）

摘要：为了减小宽带激光调频连续波测量中的色散失配效应，提出了一种外腔可调谐激光器正、反向调谐消除色散失配的方法。当外腔可调谐激光器与光纤光路结合时，系统将产生色散失配效应，表现为目标信号的谱峰展宽和峰值偏移，测距值随调谐带宽增加而变化，导致测量不稳定。为了解决这一问题，研究了外腔可调谐激光器正、反向调谐时的系统色散失配特性，结果表明，在正反向扫频时色散趋势具有对称分布的特点，建立了正反向扫频系统色散失配模型，在此基础上提出通过外腔激光器正、反向调谐实现色散对消。该方法不需要预先标定系统的色散系数，也不需要循环迭代补偿，单次测量即可完成系统色散补偿，从而为提高色散补偿效率提供了一种思路。

关 键 词：光学；激光调频连续波(frequency modulated continuous wave, FMCW)；激光测距；色散补偿；外腔可调谐激光器

中图分类号：TN249　　**文献标识码**：A

Introduction

The method of laser FMCW measurement has many advantages, such as no blind area and low SNR detection[1-6]. Compared with the current injection semiconductor laser frequency modulation technology, the frequency

Received date: 2020-06-09, **revised date**: 2020-12-25　　**收稿日期**：2020-06-09，**修回日期**：2020-12-25

Foundation items: Supported by Zhejiang Provincial Natural Science Foundation of China (LY19F050008)

Biography: XU Xin-Ke (1984-), male, Anyang, China, lecturer, Ph. D. The main research fields are photoelectric large-scale measurement, laser absolute distance measurement and laser frequency modulated continuous wave measurement. E-mail: xuxinke-123@163.com

* **Corresponding author**: E-mail: kongmjc@163.com

modulation bandwidth of the external cavity laser is large; thus, it can achieve high-resolution measurement in theory[7-10]. However, to ensure the stability and debugging convenience of the system, the optical system usually adopts the optical fiber structure. When combined with a broadband tuning light source, the dispersion mismatch effect will occur, which results in distortion of the peak profile of the target spectrum and shift of the peak position.

To eliminate the dispersion mismatch effect of the system, Zeb W. Barber analyzed the influence of optical fiber dispersion of the reference interferometer on ranging in the active chirp linearization method. The dispersion causes the beat frequency of the reference interferometer to change with the frequency modulation bandwidth, which leads to a change in the frequency modulation slope, widens the target spectrum peak and limits further improvement in the extent of the range. To solve the dispersion problem, Barber proposed introducing the chirp frequency into the beat frequency of the reference interferometer to counteract the dispersion effect [11-12]. Gan Yu *et al.* studied the phenomenon of dispersion mismatch in broadband laser frequency sweep interferometry in detail. They constructed a theoretical model of dispersion mismatch and further proposed adaptive dispersion phase compensation and chirp decomposition dispersion correction methods, the full-width at half-maximum (FWHM) of the compensated target spectrum being close to the theoretical resolution[13-15]. Dispersion mismatch also exists in swept OCT[16]. Lippok N *et al.* proposed that the group velocity dispersion coefficient of materials be measured by the fractional Fourier transform (FrFT)[17]. The group velocity dispersion coefficient and symbols are obtained by optimizing the fractional Fourier order, and then the dispersion compensation is completed. When estimating the fractional order of the FrFT, the relationship between the iteration times of the algorithm and the optimal compensation coefficient must be balanced.

The above method requires calibration of the dispersion coefficient or iterative compensation in advance. In this paper, by studying the dispersion law of the measurement system, the method of dispersion cancellation by forward and reverse tuning is proposed. It can avoid estimation of the dispersion coefficient of the system in advance or the iterative compensation process, which can improve the compensation efficiency.

1 Principles

1.1 Optical path structure of wideband tuning laser FMCW measurement

Ideally, the laser frequency performs linear tuning, and the target distance is calculated by detecting the beat frequency signal generated by the local and transmitted path light. In practice, it is difficult for lasers to achieve perfect linear tuning, which leads to broadening of the target spectrum. To eliminate this effect, an auxiliary interferometer is constructed for tuning the nonlinear correction. A structure diagram of the optical path is shown in Fig. 1.

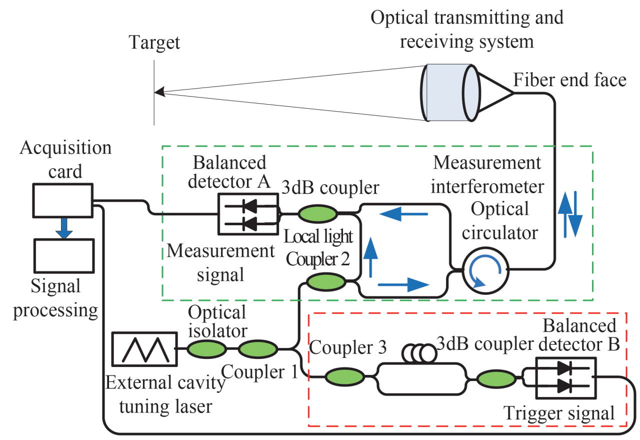

Fig. 1 Optical path diagram of laser FMCW measurement
图1 激光FMCW测量系统光路结构图

The external cavity laser is tuned linearly. The output light is divided into two channels after passing through the optical isolator and coupler 1. Part of the light passes through coupler 2. It then returns to form the beat signal with the local path light at balanced detector A. The rest of the light passes through coupler 3. It then passes through the fiber-optic Mach-Zehnder interferometer with an unequal arm length to form the auxiliary interferometer beat signal on balanced detector B. The measured beat signal is synchronously sampled by the zero-amplitude crossing point of the auxiliary interferometer signal. Then, the sampled signal is changed to a sine signal, and the frequency of the sampled signal can be calculated by a Fourier transform. The target distance is calculated by combining the optical path length of the auxiliary interferometer.

The sampled signal[13] can be expressed as:

$$I_b \propto \exp\left(j2\pi \frac{\tau_{air}}{\tau_{aux}} k\right), k = 0,1,\cdots,N-1 \quad , \qquad (1)$$

where τ_{air} and τ_{aux} are the time delays of the measurement and auxiliary interferometers, respectively. When the time delay of the auxiliary interferometer is known by calibration, the optical path of the target can be obtained by FFT of the sampled signal.

1.2 Study on the method of dispersion cancellation of the laser FMCW system

In practice, due to the use of a broadband tuning light source, it is necessary to consider the influence of optical fiber dispersion[18] of the auxiliary interferometer on the measurement. Then, the beat frequency formed by the auxiliary interferometer is as follows[11]:

$$\omega_b = \mu\beta_1 R_{aux} \rightarrow \omega_b = \mu'\beta_1 R_{aux}\left(1 + \mu\frac{\beta_2}{\beta_1}t\right), \qquad (2)$$

where

$$\mu' = \frac{\mu}{1 + \mu\beta_2 R_{aux}} = \mu\left(1 - \mu\beta_2 R_{aux} + O\left(\mu\beta_2 R_{aux}\right)^n\right), (3)$$

where R_{aux} denotes the fiber length of the auxiliary interferometer and μ is the slope of the linear tuning. $\beta_1 = 1/v_g$, and v_g denotes the group velocity. The dispersion coefficient is $\beta_2 = d\beta_1 / d\omega$. $O(\zeta)^n$ refers to an error of order ζ^n.

After the measurement signal is resampled by the signal clock of the auxiliary interferometer, the measurement beat frequency is derived as follows.

The measurement optical path is primarily in air, and the dispersion coefficient of air can be ignored. Therefore, the ratio of the time delay by the measurement and auxiliary interferometer can be expressed as Eq. 4:

$$\begin{aligned} \text{ratio} &= \frac{\tau_{\text{air}}}{\tau_{aux} + \Delta\tau_{\text{aux}}} \\ &= \frac{\tau_{\text{air}}}{\tau_{\text{aux}}} \frac{1}{1 + \frac{\Delta\tau_{\text{aux}}}{\tau_{\text{aux}}}} \\ &= \frac{\tau_{\text{air}}}{\tau_{\text{aux}}} \left[1 - \frac{\Delta\tau_{\text{aux}}}{\tau_{\text{aux}}} + O\left(\frac{\Delta\tau_{\text{aux}}}{\tau_{\text{aux}}} \right)^n \right] \end{aligned} \quad . \quad (4)$$

Because $\Delta\tau_{\text{aux}} / \tau_{\text{aux}} \ll 1$, the higher-order terms in Eq. 4 can be ignored with a negligible loss in accuracy. The higher-order terms of Eq. 4 are denoted by $O(\zeta)^n$.

Here,

$$\frac{\Delta\tau_{\text{aux}}}{\tau_{\text{aux}}} = \frac{\beta_2 2\pi\mu t}{\beta_1} = 2\pi \frac{\beta_2}{\beta_1} k \quad , \quad (5)$$

where $\Delta\tau_{\text{aux}}$ denotes the time delayed variation on the auxiliary interferometer caused by the fiber dispersion effect. After deducing the above process, the sampled signal is as follows[13]:

If $\mu < 0$,

$$I_b = (P_T P_L \eta_H)^{1/2} \cos\left[2\pi \left(\frac{\tau_{\text{air}}}{\tau_{\text{aux}}} k - \frac{\tau_{\text{air}}}{2\tau_{\text{aux}}} 2\pi \left| \frac{\beta_2}{\beta_1} \right| k^2 \right) \right], (6)$$

If $\mu > 0$,

$$I_b = (P_T P_L \eta_H)^{1/2} \cos\left[2\pi \left(\frac{\tau_{\text{air}}}{\tau_{\text{aux}}} k + \frac{\tau_{\text{air}}}{2\tau_{\text{aux}}} 2\pi \left| \frac{\beta_2}{\beta_1} \right| k^2 \right) \right], (7)$$

where, P_T, P_L and η_H represent the transmitted light, local light power and heterodyne interference efficiency, respectively.

To reduce the dispersion effect, we proposed a method of dispersion cancellation by forward and reverse tuning. The principle is as follows.

The Hilbert transform[19] is used to extract the phase of the measured signal under forward and reverse tuning, and phase unwrapping is carried out. Furthermore, the phase of the signal for dispersion elimination can be averaged by summing the phases of the two signals. The formula is as follows:

$$\begin{aligned} \varphi_{\text{aver}} &= \frac{\varphi_{\text{up}} + \varphi_{\text{down}}}{2} \\ &= \frac{\left[j\left(2\pi \frac{\tau_{\text{air}}}{\tau_{\text{aux}}} k - \pi\delta_{\text{disp}} k^2 \right) \right] + \left[j\left(2\pi \frac{\tau_{\text{air}}}{\tau_{\text{aux}}} k + \pi\delta_{\text{disp}} k^2 \right) \right]}{2} \\ &= j\left(2\pi \frac{\tau_{\text{air}}}{\tau_{\text{aux}}} k \right) \end{aligned}, (8)$$

where $\delta_{\text{disp}} = \frac{\tau_{\text{air}}}{\tau_{\text{aux}}} 2\pi \left| \frac{\beta_2}{\beta_1} \right|$. Use Eq. (8) to reconstruct the measured signal:

$$I_{b1} = \left(P_T P_L \eta_H \right)^{\frac{1}{2}} \exp\left[j\left(2\pi \frac{\tau_{\text{air}}}{\tau_{\text{aux}}} k \right) \right] \quad . \quad (9)$$

Then, Eq. (9) is the measured signal after eliminating the influence of dispersion, and the target distance can be obtained by further ChirpZ[20] transformation of the signal. The ChirpZ transform can be used to subdivide the frequency spectrum. Its effect is equivalent to the zero filling Fourier transform, but the algorithm is more efficient.

2 Experiment and results

The external cavity laser was set to triangle wave tuning mode. It tuned from 1552 nm to 1542 nm (corresponding to forward tuning) and from 1552 nm to 1562 nm (corresponding to reverse tuning). The output power and tuning speed of the laser were 1.5 mW and 100 nm/s, respectively. The optical path of the auxiliary interferometer was 220 m. The target was placed on an air flotation optical platform. The acquired time domain measured signal diagram is shown in Fig. 2. The spectrum of the measured signal after application of the Fourier transform is shown in Fig. 3. The optical path of the fiber end face was 4.524271 m, and part of the target in air is shown in the diagram.

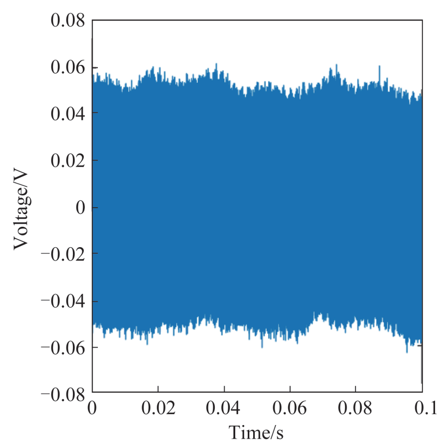

Fig. 2 Time domain of the measured signal
图 2 测量信号时域图

To study the dispersion effect of the measurement system, the measured signal formed by forward and reverse tuning of the laser was divided into five sections. Then, the ChirpZ transformation was carried out for each section of the signal, and the corresponding distance was calculated. The results are shown in Fig. 4. In the case of forward tuning, the ranging value of the target increased linearly with increasing tuning range. In the case of reverse tuning, the ranging value decreased linearly with increasing tuning range. The above phenomena were caused by dispersion mismatch, which resulted in the spectral peak of the target shifting with increasing

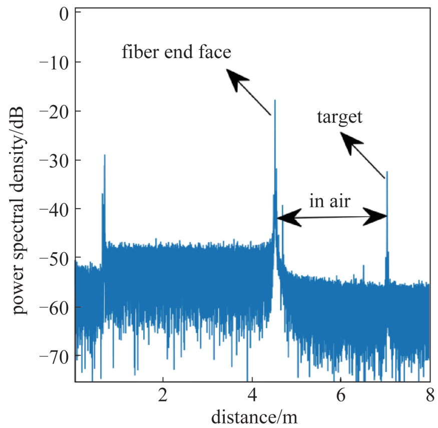

Fig. 3 Frequency domain of the measured signal
图3 测量信号频域图

tuning range.

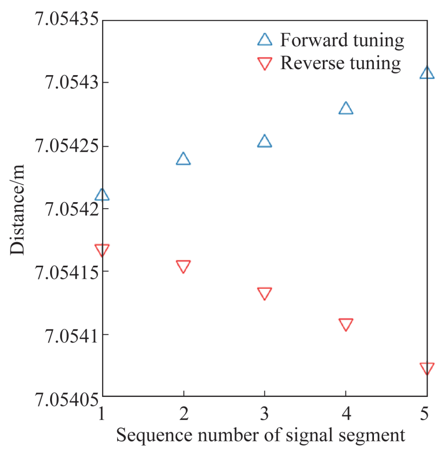

Fig. 4 Ranging value of the measured signal in different sections
图4 测量信号不同段的测距值

A Hilbert transform was used to extract the phase of the measured signal under the conditions of forward and reverse tuning. Then, the phase was unwrapped and fitted linearly. Figure 5 shows that the residual phase was a curved line that opened upward in the case of forward tuning, indicating that the beat frequency was not a constant value and changed with the tuning range. The residual phase after linear fitting of the measured signal phase in the case of reverse tuning is shown in Fig. 6. As shown, the residual phase appeared as a downward curved line. The phase of dispersion cancellation by forward and reverse tuning is shown in Fig. 7. The residual phase fluctuated around the value of zero, indicating that the dispersion effect of the measurement system was eliminated.

The measured signal was reconstructed by the phase of dispersion cancellation and divided into five sections. Then, the target distance of each section was extracted by the ChirpZ transform. The results are shown in Fig. 8. Clearly, the ranging value (green star symbol in the figure) remained basically horizontal with increasing tuning range, indicating that the system dispersion was eliminated.

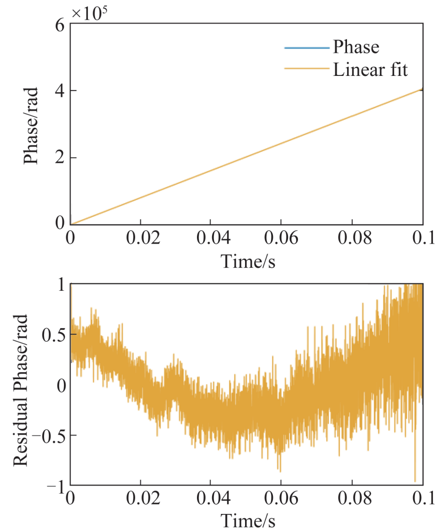

Fig. 5 Residual phase by forward tuning
图5 正向调谐的残余相位

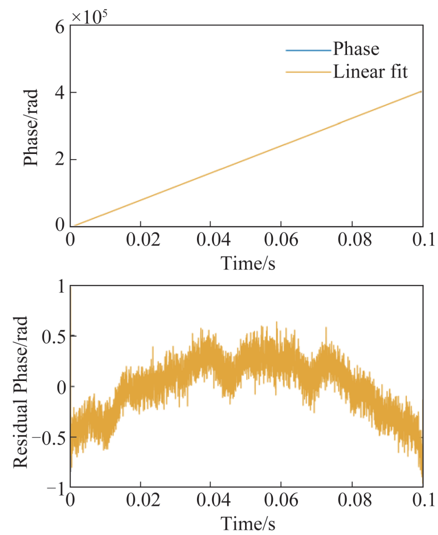

Fig. 6 Residual phase by reverse tuning
图6 反向调谐的残余相位

The whole measured signal after dispersion cancellation was extracted by the ChirpZ transform. The distance profile of the target peak before and after dispersion cancellation is shown in Fig. 9. The target peak of the forward and reverse tuning had some degree of distortion, which was caused by system dispersion. The distortion of the target peak (green solid line) after dispersion cancellation was little.

3 Conclusions

In this paper, an external cavity tunable laser FMCW system is constructed. The theoretical model of dispersion mismatch is established. The theoretical and experimental results show that the beat frequency of the measured signal changes with time due to dispersion, which leads to the distortion of the target spectrum peak profile and measurement instability. To reduce the influ-

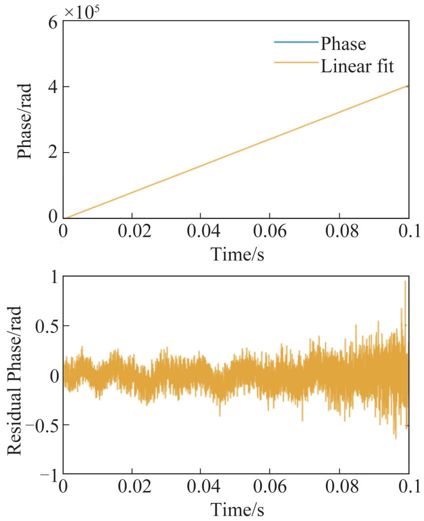

Fig. 7 Residual phase of dispersion cancellation by forward and reverse tuning
图7 正反向调谐色散对消后的残余相位

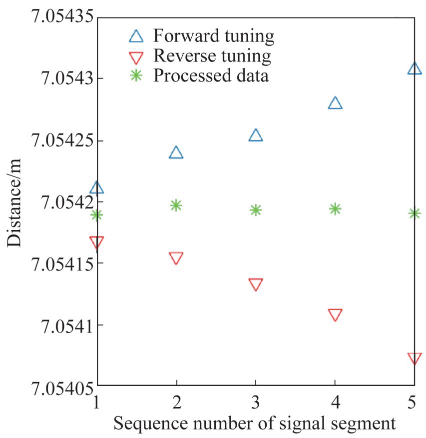

Fig. 8 Ranging value under the condition of forward and reverse tuning and after dispersion cancellation
图8 正反向调谐色散对消后的测距值

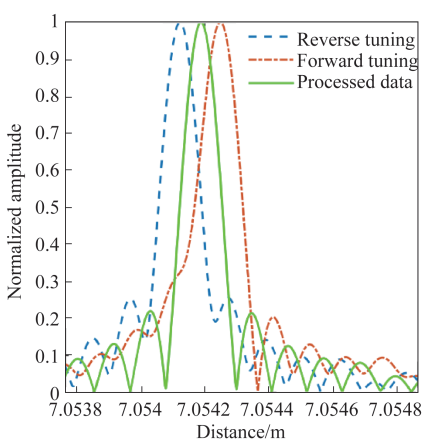

Fig. 9 The distance profile of the target peak before and after dispersion cancellation
图9 系统色散对消前后的目标距离峰轮廓

ence of dispersion, a dispersion mismatch model of the forward and reverse tuning of the external cavity laser is established. It is found that the dispersion has symmetry under forward and reverse tuning. According to this characteristic, dispersion cancellation is realized by summing and averaging the phases of the forward and reverse tuned signals. The advantage of this method is that it does not require estimation of the dispersion coefficient nor the carrying out of iterative compensation. The measurement is completed by a single compensation, which can improve the efficiency of the dispersion compensation.

References

[1] Zheng J. Analysis of optical frequency-modulated continuous-wave interference[J]. *Appl. Opt.*, 2004, **43**(21):4189-4198.
[2] Iiyama K, Matsui S I, Kobayashi T, *et al.* High-resolution fmcw reflectometry using a single-mode vertical-cavity surface-emitting laser[J]. *IEEE Photon. Technol. Lett.*, 2011, **23**(11):703-705.
[3] Mateo A B, Barber Z W. Precision and accuracy testing of FMCW ladar-based length metrology[J].*Appl.Opt.*,2015,**54**(19):6019-6024.
[4] Hariyama T, Sandborn P A M, Watanabe M, *et al.* High-accuracy range-sensing system based on FMCW using low-cost VCSEL[J]. *Opt. Express*, 2018, **26**(7): 9285-9297.
[5] Deng Z W, Liu Z G, Jia X Y, *et al.* Real-time dynamic absolute ranging with frequency scanning interferometry using a robust Monte-Carlo-based particle filter[J], *Appl. Opt.*, 2019, **58**(25): 6865-6872.
[6] Jia X, Liu Z, Deng Z, *et al.* Dynamic absolute distance measurement by frequency sweeping interferometry based Doppler beat frequency tracking model[J]. *Opt. Commun.*, 2019, **430**:163 - 169.
[7] Soller B, Gifford D, Wolfe M, *et al.* High resolution optical frequency domain reflectometry for characterization of components and assemblies[J]. *Opt. Express*, 2005, **13**(2):666-674.
[8] Dale J, Hughes B, Lancaster A J, *et al.* Multi-channel absolute distance measurement system with sub ppm-accuracy and 20 m range using frequency scanning interferometry and gas absorption cells[J]. *Opt. Express*, 2014, **22**(20):24869-24893.
[9] Shi G, Zhang F, Qu X, *et al.* High-resolution frequency-modulated continuous-wave laser ranging for precision distance metrology applications[J]. *Opt. Eng.*, 2014, **53**(12):122402-1-6.
[10] Shi G , Wang W , Zhang F. Precision improvement of frequency-modulated continuous-wave laser ranging system with two auxiliary interferometers[J]. *Opt. Commun.*, 2018, **411**:152-157.
[11] Barber Z W, Babbitt W R, Kaylor B, *et al.* Accuracy of active chirp linearization for broadband frequency modulated continuous wave ladar[J]. *Appl. Opt.*, 2010, **49**(2):213-219.
[12] Roos P A, Reibel R R, Berg T, *et al.* Ultrabroadband optical chirp linearization for precision metrology applications [J]. *Opt. Lett.*, 2009, **34**(23):3692-3694.
[13] Xu X K, Liu G D, Liu B G, *et al.* Research on the fiber dispersion and compensation in large-scale high-resolution broadband frequency modulated continuous wave laser measurement system [J]. *Opt. Eng.*, 2015, **54**(7):074102-1-074102-8.
[14] Liu G D, Xu X K, Liu B G, *et al.* Dispersion compensation method based on focus definition evaluation functions for high-resolution laser frequency scanning interference measurement [J]. *Opt. Commun.*, 2016, **386**:7-64
[15] Lu C, Liu G D, Liu B G, *et al.* Method based on chirp decomposition for dispersion mismatch compensation in precision absolute distance measurement using swept-wavelength interferometry [J]. *Opt. Express*, 2015, **23**(25):31662-71
[16] Huang D, Swanson E A, Lin C P, *et al.* Optical coherence tomography[J]. *Science*, 1991, **254**(5035):1178-1181.
[17] Lippok N, Coen S, Nielsen P, *et al.* Dispersion compensation in Fourier domain optical coherence tomography using the fractional Fourier transform[J]. *Opt. Express*, 2012, **20**(21): 23398-23413.
[18] Agrawal G P. *Nonlinear Fiber Optics*, *third ed.* [M]. Academic Press, San Diego, 2001.
[19] Ahn T J, Lee J Y, Kim D Y. Suppression of nonlinear frequency sweep in an optical frequency-domain reflectometer by use of Hilbert transformation[J]. *Appl. Opt.*, 2005, **44**(35):7630-7634.
[20] Rabiner L, Schafer R, Radar C. The ChirpZ transform algorithm[J]. *IEEE Transaction On Audio and Electro Acoustics*, 1969, **17**(2): 86-92.